Experimental determination of the quasiparticle energy distribution function in optically perturbed superconducting films

F. Jaworski and W. H. Parker
Department of Physics, University of California, Irvine, California 92717
(Received 1 March 1979)

The nonequilibrium quasiparticle energy distribution function of optically irradiated superconductors is obtained from an analysis of the current-voltage curve of superconducting-insulator-superconductor tunnel junctions. The result is in excellent agreement with the numerical solution of the appropriate kinetic equations.

Measurements on superconductor-insulator-superconductor tunnel junctions can be used to obtain valuable information about the energy distribution of quasiparticles in a superconductor perturbed from equilibrium by some external mechanism. Chang and Scalapino[1] have shown that, in principle, the exact energy distribution function of the quasiparticles in the nonequilibrium state of a superconductor can be obtained from measurements of the change in the current through tunnel junctions biased at constant voltage. The change in the current produced by the application of an external perturbation is related to the quasiparticle distribution function through an integral equation. Proper numerical solution of this linear integral equation yields the exact distribution function. This process of obtaining the distribution function from changes in the current-voltage characteristics of the tunnel junction had not previously been successfully used in the investigation of the nonequilibrium properties of superconductors. Other investigators[2] have been able to fit qualitatively the change produced by some external mechanism in the $I(V)$ characteristic of tunnel junctions by the assumption of several functional forms or parameters for the nonequilibrium quasiparticle distribution function and the selection of that function or parameter which best reproduces the data when inserted into the integral equation.

In this paper, we report an analysis of the changes in the $I(V)$ characteristic of optically perturbed superconducting tunnel junctions which yields the exact quasiparticle energy distribution function, and compare the results of this analysis with various theoretical models for nonequilibrium superconductors. The results are in reasonable agreement with the modified heating model suggested by Parker,[3] and in better agreement with the numerical solution of the kinetic equations obtained by Chang and Scalapino.[4]

The experiment is relatively straight forward. Sn-*I*-Sn tunnel junctions of area approximately 0.4×0.4 mm are fabricated on glass substrates and immersed in liquid helium. The superconducting films are typically 1000 Å thick. The junctions are illuminated on one side with light that is mechanically modulated at 83 Hz. The exciting optical radiation is spatially homogeneous over the dimensions of the junction. The junction is biased at a constant voltage using a dynamic constant voltage source.[5] The change in the current through the junction at the modulation frequency is detected by a lock-in amplifier. A small magnetic field is applied if necessary to suppress the Josephson currents. The optical modulation is sufficiently weak that the spatial instabilities thought to occur with strong perturbations should not be a factor in this measurement.[6]

Even though the junction is illuminated on only one side, we assume that the entire junction (both films) is uniformly perturbed by the optical radiation. The acoustic mismatch between the superconductor and the substrate or liquid helium, and the thickness of the films, result in the trapping of the recombination phonons within the superconductor. The recombination phonons produced in the illuminated film easily propagate through the oxide barrier and excite quasiparticles in the unilluminated film.[7]

We follow the analysis suggested by Chang and Scalapino[1] to extract information on the distribution function from the measured current-voltage curves. It is convenient to introduce an effective excess tunnel current

$$\delta I_E = I(V;\Delta_L^*;\Delta_R^*;f_L^*(E);f_R^*(E)) - I(V;\Delta_L^*;\Delta_R^*;f_L(E);f_R(E)) \quad , \tag{1}$$

where the superscript asterisk denotes the nonequilibrium state, $\Delta_{R,L}$ denotes the energy gap in the right and left films forming the junction respectively, $f_{R,L}$ denotes the quasiparticle energy distribution function in the right and left films, and V denotes the potential difference across the insulator. This effective excess current is not the excess current measured in the experiment. The measured excess current is

$$\delta I = I(V;\Delta_{R,L}^*;f_{R,L}^*) - I(V;\Delta_{R,L};f_{R,L}) \quad .$$

While δI_E is not the directly measured quantity, it is introduced here because (a) it depends only on the

change of the distribution function and not on the change of the energy gap, and (b) it simplifies somewhat the numerical computations described below. The relationship between δI_E and δI will be discussed shortly.

From Chang and Scalapino, the effective excess current is the sum of three contributions $\delta I_E = \delta I_E^a + \delta I_E^b + \delta I_E^c$ where

$$\delta I_E^a = \frac{1}{Re}\int_{\Delta_L^*}^{\infty} dE\, \frac{E(E+eV)\Theta(E+eV-\Delta_R^*)}{\{(E^2-\Delta_L^{*2})[(E+eV)^2-\Delta_R^{*2}]\}^{1/2}}[\delta f_L(E)-\delta f_R(E+eV)]\ , \tag{2a}$$

$$\delta I_E^b = -\frac{1}{Re}\int_{\Delta_L^*}^{\infty} dE\, \frac{E(E-eV)\Theta(E-eV-\Delta_R^*)}{\{(E^2-\Delta_L^{*2})[(E-eV)^2-\Delta_R^{*2}]\}^{1/2}}[\delta f_L(E)-\delta f_R(E-eV)]\ , \tag{2b}$$

$$\delta I_E^c = -\frac{1}{Re}\int_{\Delta_L^*}^{\infty} dE\, \frac{E(eV-E)\Theta(eV-E-\Delta_R^*)}{\{(E^2-\Delta_L^{*2})[(eV-E)^2-\Delta_R^{*2}]\}^{1/2}}[\delta f_L(E)+\delta f_R(eV-E)]\ , \tag{2c}$$

and R is the normal-state resistance, e the electron charge, and Θ the Heaviside step function $[\Theta(x<0)=0,\ \Theta(x>0)=1]$. Also

$$\delta f_{L,R}(E) \equiv f_{L,R}^*(E) - f_{L,R}(E)\ .$$

The effective excess current can be obtained from the experimentally measured change in the current by expanding the effective excess current in a Taylor expansion and calculating the first-order correction term assuming an equilibrium BCS superconductor,

$$\delta I_E = \left[\delta I + \frac{\delta I}{\delta\Delta}\right]_{V,f}\delta\Delta + \cdots\ . \tag{3}$$

Some idea of the difference between δI_E and δI can be obtained from Fig. 1. Figure 1 compares δI_E and δI for a small change in the energy gap $\delta\Delta$ where both δI_E and δI have been calculated for a BCS superconductor using an effective temperature T^* to characterize the nonequilibrium distribution function.[3] Note that below the voltage 2Δ the effective excess current is very nearly the same as the measured excess current. In this region of the I-V curve any small errors in the first-order correction term should be unimportant. However, above the gap, the difference between the measured and effective excess currents become comparable to, or even larger than, the measured excess current. Since this difference for $V > 2\Delta$ is sensitive to the exact value of the energy gap, and any possible smearing or energy dependence of the gap, the accuracy of the correction of the data obtained at voltages above 2Δ is doubtful. Therefore, only data taken at voltages below 2Δ will be considered in the analysis.

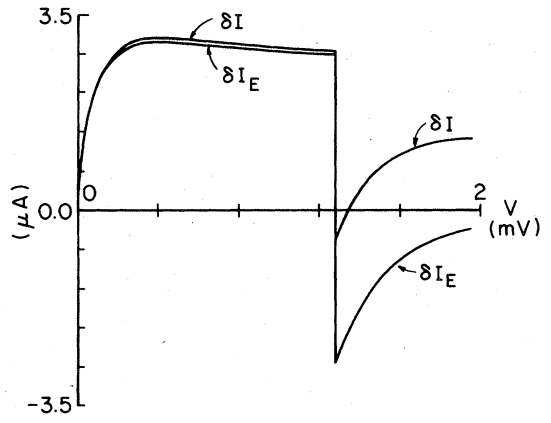

FIG. 1. Change in current vs the voltage across a Sn-I-Sn junction. The upper curve is $\delta I = I(V,f(T^*),\Delta^*) - I(V,f(T),\Delta)$ while the lower curve is $\delta I_E = I(V,f(T^*),\Delta) - I(V,f(T),\Delta^*)$. Both of these curves are calculated within the BCS model.

Another reason to restrict this analysis to changes in the current below a voltage of 2Δ is to avoid the possibility of the bias current itself producing a nonequilibrium condition among the quasiparticles. For voltages above 2Δ the current is sufficient to inject a significant number of quasiparticles into the superconductors, especially at low temperatures. Below a voltage of 2Δ, the bias current can be orders of magnitude smaller, especially at low temperatures.

Since we are assuming that the two superconducting films composing the tunnel junction are equally perturbed, Eqs. (1) and (2) reduce to

$$\delta I_E = I(V;\Delta^*;f^*) - I(V;\Delta^*;f)$$

and

$$\delta I_E^a = \frac{1}{Re}\int_{\Delta^*}^{\infty} dE\, \rho(E)\rho(E+V)\Theta(E+eV-\Delta^*) \times [\delta f(E)-\delta f(E+eV)]\ , \tag{4a}$$

$$\delta I_E^b = -\frac{1}{Re}\int_{\Delta^*}^{\infty} dE\, \rho(E)\rho(E-eV)\Theta(E-eV-\Delta^*) \times [\delta f(E)-\delta f(E-eV)]\ , \tag{4b}$$

$$\delta I_E^c = -\frac{1}{Re}\int_{\Delta^*}^{\infty} dE\, \rho(E)\rho(eV-E)\Theta(eV-E-\Delta^*) \times [\delta f(E)+\delta f(eV-E)]\ , \tag{4c}$$

where right and left sides are no longer denoted, and $\rho(E)$ is the BCS density of states characterized by an energy gap of Δ^*.

Combining the three integrals for the current above and below $2\Delta^*$ yields:

$$\delta I_E(V) = \delta I_E^a + \delta I_E^b = \frac{1}{Re}\int_{\Delta^*}^{\infty} dE\, G(E,V)\delta f(E), \quad V < 2\Delta^* , \tag{5a}$$

where

$$G(E,V) = \rho(E)\{\rho(E+eV)[1+\Theta(E+eV-\Delta^*)] - 2\rho(E-eV)\Theta(E-eV-\Delta^*)\} \tag{5b}$$

and

$$\delta I_E(V) = \delta I_E^a + \delta I_E^b + \delta I_E^c = \frac{1}{Re}\int_{\Delta^*}^{\infty} dE\, F(E,V)\delta f(E), \quad V \geq 2\Delta^* , \tag{6a}$$

where

$$F(E,V) = 2\rho(E)[\rho(E+eV) - \rho(E-eV)\Theta(E-eV-\Delta^*) - \rho(eV-E)\Theta(eV-E-\Delta^*)] . \tag{6b}$$

Equations (5) and (6) are integral equations which relate the effective excess current δI_E to the change in the distribution function $\delta f(E)$. The integral equations can be written in matrix form by replacing the continuous variable E with a finite set of values separated by ΔE.

$$\delta I_E = \begin{cases} \sum_E G(E,V)\delta f(E)(\Delta E), & V < 2\Delta^* , \quad (7a) \\ \sum_E F(E,V)\delta f(E)(\Delta E), & V \geq 2\Delta^* , \quad (7b) \end{cases}$$

or

$$\underline{\delta I_E} = \begin{cases} \underline{G}(E,V)\underline{\delta f}(E), & V < 2\Delta^* , \quad (7c) \\ \underline{F}(E,V)\underline{\delta f}(E), & V \geq 2\Delta^* . \quad (7d) \end{cases}$$

The change in the distribution function can in principle be obtained by multiplying either Eq. (7c) or (7d) by $\underline{G}^{-1}$ or $\underline{F}^{-1}$ respectively. However, the three singularities within $\underline{G}$ and $\underline{F}$ arising from the normalized density-of-states factors make numerical evaluation difficult. An appropriate change of variable can remove one but not all three of the singularities in $\underline{G}$ and $\underline{F}$.

Numerical evaluation becomes easier if the following procedure is followed.[7] The integration domain of Eq. (5) is divided into a series of N finite segments

$$\delta I_E(V) = \frac{1}{Re}\sum_i^N \int_{E_i}^{E_{i-1}} dE\, G(E,V)\delta f(E) . \tag{8}$$

$\delta f(E)$ can be expressed as a linear interpolation between the endpoints E_i and E_{i+1}, i.e.,

$$\delta f(E) = \delta f(E_i)\left(\frac{E_{i+1}-E}{E_{i+1}-E_i}\right) + \delta f(E_{i+1})\left(\frac{E-E_i}{E_{i+1}-E_i}\right) . \tag{9}$$

Combining Eqs. (8) and (9) yields Eq. (10) where the integrals that must be evaluated have at most a single singularity that can be removed by an appropriate change of variable.

$$\delta I_E(V) = \frac{1}{Re}\sum_{i=1}^{N+1} G_1(E_i,V)\delta f(E_i), \quad V < 2\Delta^* , \tag{10a}$$

where

$$G_1(E_i,V) = \int_{E_i}^{E_{i+1}} G(E,V)\left(\frac{E_{i+1}-E}{E_{i+1}-E_i}\right)\Theta(N-i)\,dE + \int_{E_{i-1}}^{E_1} G(E,V)\left(\frac{E-E_{i-1}}{E_i-E_{i-1}}\right)\Theta(i-2)\,dE . \tag{10b}$$

Similarly for voltages greater than $2\Delta^*$,

$$\delta I_E(V) = \frac{1}{Re}\sum_{i=1}^{N+1} F_1(E_i,V)\delta f(E_i), \quad V \geq 2\Delta^* , \tag{11a}$$

where

$$F_1(E,V) = \frac{1}{Re}\left[\int_{E_i}^{E_{i+1}} dE\, F(E,V)\left(\frac{E_{i+1}-E}{E_{i+1}-E_i}\right)\Theta(N-i) + \int_{E_{i-1}}^{E_i} F(E,V)\left(\frac{E-E_{i-1}}{E_i-E_{i-1}}\right)\Theta(i-2)\,dE\right] \tag{11b}$$

Equation (10a) can be written as a matrix equation

$$\delta I_E = \underline{G}_1\underline{\delta f}(E) . \tag{12}$$

This equation can in principle be solved for $\delta f(E)$ by finding $(\underline{G}_1)^{-1}$, a square matrix. Recall that δI_E is obtained from the experimental data by applying a small correction and $\underline{G}_1$ is obtained from numerical integration of Eqs. (10). We will use only Eq. (10) to obtain $\delta f(E)$ because the useful data obtained from the tunnel junctions is limited to the region $V < 2\Delta$ for the reasons mentioned earlier.

Even though the elements of the matrix $\underline{G}_1$ can be obtained numerically, there is still a difficulty in obtaining $\delta f(E)$ from Eq. (10). $\underline{G}_1$ is an ill-conditioned matrix.[8] This means that $\delta f(E)$ can be obtained

from $(\underline{G}_1)^{-1}\underline{\delta I}_E$ only if δI_E is obtained with negligible error. Any error in δI_E is sufficiently amplified by the ill-condition of $\underline{G}_1$ that the numerical solution of Eq. 12 for $\delta f(E)$ is erratic and meaningless. Some insight into the origin of the ill-condition can be obtained from an examination of the family of curves in Fig. 2 where $G_1(E,V)$ is plotted against E with V as a parameter. A large spike in the function occurs whenever $E=\Delta^*+eV$ and this spike dominates the $G_1(E,V)$ curve. To obtain a satisfactory representation of the functions $G_1(E,V)$, the set of values for the variable E should include several values near the cusp. Since the matrix $\underline{G}_1$ must be square in order to be inverted, it is difficult to obtain a satisfactory representation of $\underline{G}_1$.

However, it is still possible to obtain $\delta f(E)$ to an accuracy commensurate with the data. The function $\delta f(E)$ can be expanded in a series of appropriate functions with coefficients to be determined from a numerical fit to the data. Let

$$\delta f(E)=a_1g_1(E)+a_2g_2(E)+\cdots+a_pg_p(E)\ , \quad (13)$$

or

$$\underline{\delta f}(E)=\underline{g}(E)\underline{a}\ , \quad (14)$$

where

$$\underline{g}(E)=\begin{pmatrix} g_1(E_1) & \cdots & g_p(E_1) \\ \vdots & & \vdots \\ g_1(E_N) & \cdots & g_p(E_N) \end{pmatrix}$$

and

$$\underline{a}=\begin{pmatrix} a_1 \\ \vdots \\ a_p \end{pmatrix}\ .$$

Combining Eqs. (12) and (14), we obtain

$$\underline{\delta I}_E=\underline{G}_1\underline{g}(E)\underline{a}\ . \quad (15)$$

The matrix $\underline{a}$ is then computed from

$$\underline{a}=\underline{A}^{-1}\underline{\delta I}_E\ , \quad (16)$$

where

$$\underline{A}=\underline{G}_1\underline{g}(E)\ .$$

The procedure for finding $\delta f(E)$ is now: (i) calculate the matrix $\underline{G}_1$, (ii) choose an appropriate set of functions $g_1(E),\ldots,g_p(E)$, (iii) calculate the coefficients $a_1\ldots a_p$ from Eq. (16), (iv) calculate $\delta f(E)$ from Eq. (14), (v) compare the calculated excess current from Eq. (12) to the measured excess current [Eq. (3)] and if the difference exceeds the experimental error, (vi) add another function to the set $g(E)$ and return to step (ii) of this procedure.

The result obtained from the application of this procedure to the data from a Sn-I-Sn tunnel junction of 4.3 Ω normal-state resistance at a bath temperature of 1.33 K and exposed to optical radiation is shown as curve B in Fig. 3 where $\delta f(E)$ is plotted against E. Curve A is the function g_1. For this calculation we chose as g_1 the difference between Fermi-Dirac func-

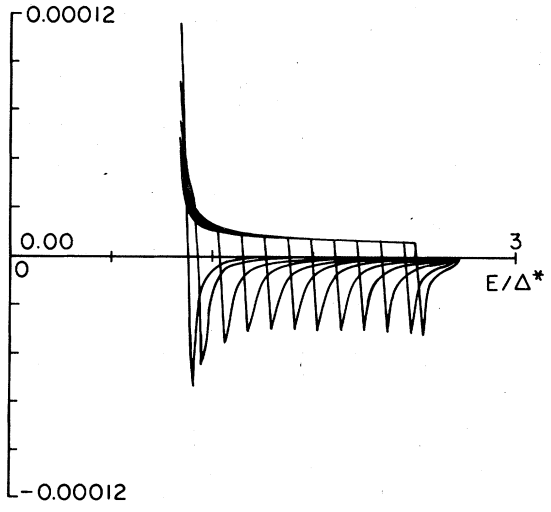

FIG. 2. Rows of the matrix $G_1(E/\Delta^*,V)$ vs E/Δ^*, the normalized quasiparticle energy. Each member of this family of curves is characterized by a value of the voltage across the junction.

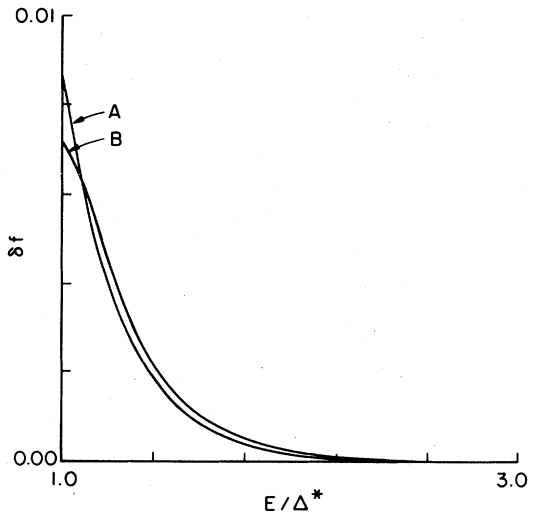

FIG. 3. Change in the quasiparticle distribution function δf vs E/Δ^*. Curve A represents $\delta f=f(T^*,E)-F(T,E)$ and curve B represents $\delta f=f^*(E)-f(T,E)$ where f is the Fermi-Dirac distribution function and f^* is the experimentally determined distribution function.

tions evaluated at the ambient temperature and an effective temperature determined from the modified heating model, i.e., $g_1 = f(T^*) - f(T)$. The coefficient a_1 in Eq. (13) was set equal to 1. We make this choice since we expect the modified heating model to be approximately correct for optically perturbed superconductors. The effective temperature T^* was calculated from the normalized excess quasiparticle number n which in turn was obtained from the change in the energy gap $\delta\Delta$ and the relation $n = \delta\Delta/2\Delta$. Published graphs in Ref. 3 relate T^* to n and T. The remaining functions in the series in Eq. (13) were E^{-n} with $n = 1, 2, \ldots$. Terms of inverse power up to 4 were necessary to fit the data to within the experimental accuracy.

The perturbation that produced the data in Fig. 3 is not small. The change in the distribution function at an energy $E \cong \Delta$ is in fact larger than the value of the equilibrium distribution function at $E \cong \Delta$. According to Fig. 3, the value of $\delta f(E)$ at $E = \Delta$ is 7×10^{-3}. At a temperature of 1.33 K and an energy of $E = \Delta$, the value of the Fermi-Dirac distribution function is 5×10^{-3}. Another way of quantitatively expressing the extent to which the superconductor is out of equilibrium is the comparison of the normalized excess quasiparticle density n to the normalized equilibrium quasiparticle density. For the data in Fig. 3, $n = 6.4 \times 10^{-3}$ while the normalized equilibrium quasiparticle density is 3.1×10^{-3}. Also the effective temperature $T^* = 1.64$ K for the data in Fig. 3 in comparison to the ambient temperature $T = 1.33$ K.

The accuracy to which the experimental data can be fit is shown in Fig. 4 where the measured excess current δI_E is plotted against the voltage across the junction as curve *B*. A calculated excess current determined from the change in the distribution function shown in Fig. 3 is also plotted as curve *B*. To within the width of the line, the actual data and the calculated curve agree. Also shown in Fig. 4 as curve *A* is the best fit to the data using the modified heating model. All three curves coincide at voltages near 2Δ but the curve calculated from the modified heating model is clearly incorrect at voltages below Δ (for Sn, $\Delta \cong 0.6$ mV).

We believe the small differences shown in Fig. 3 between the calculated nonequilibrium distribution function and a Fermi-Dirac function at an effective temperature T^* are meaningful. We have tried a variety of functions as expansion functions in Eq. (13) and while the number of required functions and their coefficients would vary with the choice of functions, we always obtained the same final result for $\delta f(E)$. Thus the choice of expansion functions does not appear to be crucial as long as the functions decrease with increasing energy. We also found that we could fit the current-voltage curve of the equilibrium (unilluminated) junction in the voltage region $0 < V < \Delta$ to within the accuracy of the data. This

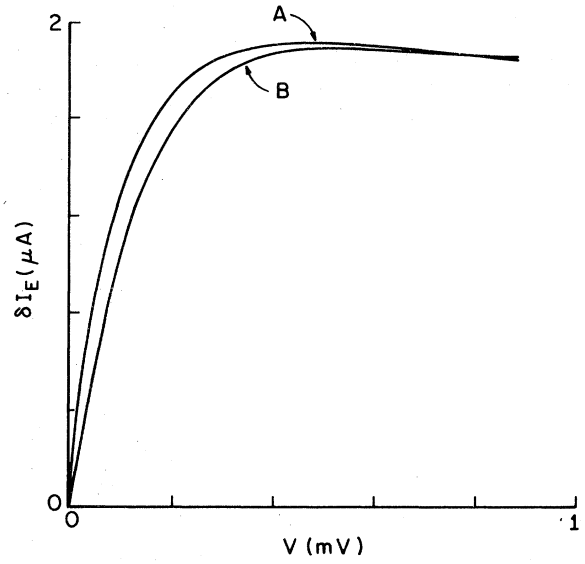

FIG. 4. Change in tunnel current δI_E vs V where $\delta I_E = I(V, \Delta^*, f^*) - I(V, \Delta^*, f)$. Curve *A* is calculated within the T^* model. Curve *B* is the experimental data. The calculated δI_E using the experimentally determined distribution function corresponds to curve *B* to within the thickness of the line.

indicates that the tunnel junction I-V curve in this voltage region was well described by BCS density of states and simple tunneling theory.

Excess tunneling currents of the kind reported by Taylor and Burstein[9] were observed at voltages $\Delta < V < 2\Delta$. It is interesting to note that these excess tunneling currents do not appear in the data displayed in Fig. 4. This suggests that the excess tunneling current in our junctions is independent of the distribution function since the data in Fig. 4 is obtained from the difference

$$\delta I = I(V, \Delta^*, f^*) - I(V, \Delta, f) \ .$$

This result is consistent with the observation of Taylor and Burstein that the type of excess tunnel current appearing in Sn-*I*-Sn junctions is approximately temperature independent.

While Fig. 3 displays the change in the quasiparticle distribution function caused by the external optical perturbation, Fig. 5 displays the quasiparticle distribution function itself obtained under the experimental conditions discussed above. Curve *B* displays the actual nonequilibrium quasiparticle distribution function $f^*(E) = \delta f + f(T,E)$ where $f(T,E)$ is the Fermi-Dirac function. Curve *A* is the Fermi-Dirac function evaluated at the effective temperature $T^* = 1.64$ which best fits the experimental data.

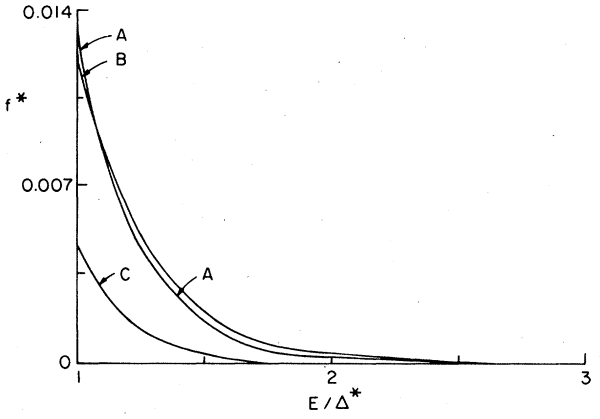

FIG. 5. Nonequilibrium quasiparticle distribution function $f^*(E)$ vs E/Δ^*. Curve B is the experimental result obtained from a Sn-I-Sn tunnel junction. Curve A is the Fermi-Dirac function evaluated at the effective temperature $T^* = 1.64$ K. Curve C is the Fermi-Dirac function evaluated at the ambient temperature $T = 1.33$.

Curve C is the Fermi-Dirac function evaluated at the ambient temperature $T = 1.33$ K.

In Fig. 6 we reproduce the calculated distribution function obtained by Chang and Scalapino who numerically have solved the kinetic equations appropriate for the nonequilibrium superconductor. They have calculated the steady-state, nonequilibrium distribution function for a superconductor irradiated by thermal phonons characterized by a temperature much greater than the bath temperature and then argue that this result should be appropriate for optically illuminated superconductors. A parameter in their calculation is the ratio of the phonon escape time τ_γ to the zero-temperature pair breaking time τ_β for a phonon of energy 2Δ. The zero-temperature pair breaking time at an energy of 2Δ for Sn is found in Kaplan *et al.*[10] The phonon escape time from the superconducting films used in the experiment is calculated from $\tau_\gamma \cong 4d/\eta c_s$ where d is the total junction thickness, η the transmissivity of phonons at the helium-superconductor interface, and c_s the speed of sound. The resulting ratio for the data reported here is $\tau_\gamma/\tau_\beta \cong 8$. Thus the experimental results should be compared to the theoretical results corresponding to ratios of $\tau_\gamma/\tau_\beta > 1$, i.e., to curve c in Fig. 6.

Also shown in Fig. 6 as the dashed curve is the result of the modified heating model for the conditions appropriate to their calculation. Note the similarities between the curves in Figs. 5 and 6. The experimentally determined nonequilibrium distribution function differs from the modified heating model in exactly the same manner as it differs from the detailed kinetic equation calculation. The principal

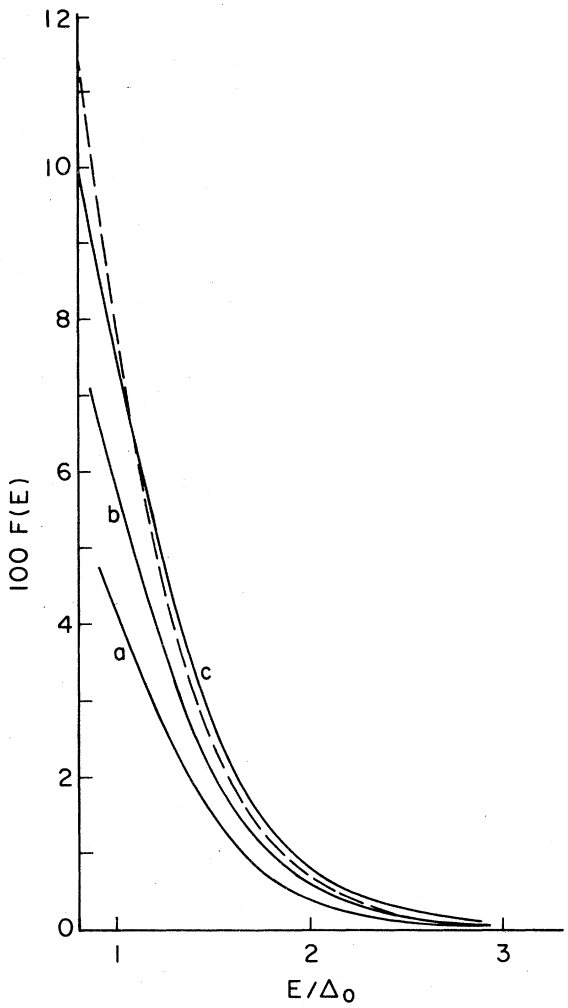

FIG. 6. $f^*(E)$ vs E/Δ_0 as calculated from the coupled kinetic equations for quasiparticles and phonons. Δ_0 is the gap at $T = 0$. The dashed curve corresponds to the best fit of the T^* model. Curves a,b,c correspond to phonon escape times of $3/5\tau_\beta$, $5/4\tau_\beta$ and $3\tau_\beta$ where τ_β is the zero-temperature pair breaking lifetime for a phonon of energy 2Δ.

difference is the reduction in the number of quasiparticles at energies very near the gap energy, and the distribution of these quasiparticles over an energy range between Δ and $\sim 2\Delta$. Physically, this implies that the excited quasiparticles lose their excess energy by some appropriate relaxation mechanism in a time comparable to or shorter than the time required for the quasiparticles to come into thermal equilibrium with the phonons. In other words, the effective recombination time is not significantly longer than the quasiparticle relaxation time. This is in agreement with the calculations of Kaplan *et al.*[10]

In summary, we have extracted the nonequilibrium

quasiparticle energy distribution function for the case of optically irradiated superconductors from an analysis of $I(V)$ curves of superconductor-insulator-superconductor tunnel junctions, and have found the result to be in excellent agreement with the numerical solution of the appropriate kinetic equations.

This research was supported by the NSF under Grant No. DMR76-23566.

[1]J. J. Chang and D. J. Scalapino, Phys. Rev. Lett. 37, 522 (1976).
[2]S. B. Kaplan, J. R. Kirtley, and D. N. Langenberg, Phys. Rev. Lett. 39, 29 (1977); H. W. Willemsen and K. E. Gray, Phys. Rev. Lett. 41, 812 (1978).
[3]W. H. Parker, Phys. Rev. B 12, 3667 (1975).
[4]J. J. Chang and D. J. Scalapino, Phys. Rev. B 15, 2651 (1977); J. J. Chang and D. J. Scalapino, IEEE Trans. Magn. 13, 747 (1977).
[5]B. L. Blackford, Rev. Sci. Instrum. 42, 1198 (1971); Irwin L. Singer, Ph.D. thesis (Indiana University, 1976) (unpublished).
[6]D. J. Scalapino and B. A. Huberman, Phys. Rev. Lett. 39, 1365 (1977).
[7]J. J. Chang (private communication).
[8]A. M. Cohen, *Numerical Analysis* (Wiley, New York, 1973).
[9]B. N. Taylor and S. Burstein, Phys. Rev. Lett. 10, 14 (1963).
[10]S. B. Kaplan, C. C. Chi, D. N. Langenberg, S. S. Chang, S. Jafarey, and D. J. Scalapino, Phys. Rev. B 14, 4854 (1976).